Molecular Therapy
Methods & Clinical Development
Original Article

Analytical band centrifugation for the separation and quantification of empty and full AAV particles

Harshit Khasa,[1] Greg Kilby,[1] Xiaoyu Chen,[1] and Chunlei Wang[1]

[1]Analytical Sciences, BioPharmaceuticals Development, BioPharmaceuticals R&D, AstraZeneca, One MedImmune Way, Gaithersburg, MD 20878, USA

Analytical band centrifugation (ABC) was first developed for the separation of macromolecules in centrifugation cells ~60 years ago. Since its development, ABC has been predominantly utilized to study macromolecular interactions or chemical reactions between two solutions *in situ* upon mixing. In this current study, we evaluated ABC separations on modern analytical ultracentrifugation (AUC) instruments for therapeutic adeno-associated viruses (AAVs). ABC provided sufficient separation between the genome-containing full AAV particle and the empty AAV capsid, which need to be controlled during the manufacturing process. Because ABC produces a physical separation, no complex algorithm or sophisticated software is needed to process the experimental raw data. ABC profiles, dubbed "centrifugrams", can be analyzed with a similar approach as typically used for electrophoretic separations to produce relative percent area. Sedimentation coefficients (*s*) of analytes can also be determined from ABC. The relative area percent and *s* value obtained in ABC experiments were shown to be consistent with those determined by conventional sedimentation velocity AUC (SV-AUC). Additionally, the separation and quantification by ABC were found to be reproducible and did not appear to be sensitive to experimental variations of initial rotor temperature or cell misalignment. The robustness of the separation, ease of data processing, and universal applicability for analysis of different AAV serotypes make ABC a promising technique for routine analysis of empty and full AAV particle composition in therapeutic products.

INTRODUCTION

Adeno-associated virus (AAV) vector is an emerging platform for *in vivo* gene therapy delivery.[1] During AAV production, empty capsids with no packed genome are commonly observed impurities that have been reported to potentially impact safety and efficacy of therapeutic AAVs.[2,3] Therefore, they are proactively monitored during process development. Multiple methods have been explored to determine the percentage of empty capsids in AAV samples.[4] Sedimentation velocity analytical ultracentrifugation (SV-AUC) is one of the state-of-art methods employed for this analysis, as it provides high resolution and wide applicability for analysis of AAVs of different serotypes.[5]

SV-AUC experiments study the sedimentation of a homogeneous solution under a centrifugal force. The sedimentation of macromolecules results in their spatial redistribution, which is recorded by a concentration detector scanning a defined radius range. The observed concentration profiles can be theoretically described by the partial differential equation known as the Lamm equation.[6] Numerical solutions to the Lamm equation can be computed to obtain hydrodynamic information of the macromolecules being analyzed.[6] In AAV applications, empty capsids have lower density and, therefore, sediment slower than full AAV particles. Thus, their concentration can be deconvoluted to provide the empty-full composition of the AAV samples being studied.

More than an orthogonal and versatile characterization tool, SV-AUC is increasingly being evaluated for its potential application as a routine release test for therapeutic macromolecules. Arthur et al.[7] studied the sources of SV-AUC method variability and identified cell misalignment as the major contributing factor. Pekar and Sukumar[8] reported that centerpiece quality and data analysis variables could affect precision of protein aggregation results determined by SV-AUC. Zhao et al.[9] initiated a 67-laboratory study to show a high level of great precision and accuracy obtained for the sedimentation coefficient and aggregation percentage in a bovine serum albumin (BSA) standard. External calibration references for scan velocity, temperature, radial magnification, and data acquisition elapsed time correction were demonstrated to further reduce method variability. Savelyev et al.[10] outlined challenges for potential good manufacturing practice validation of AUC methods and highlighted the need for auditable software for data acquisition, processing, and reporting.

Analytical band centrifugation (ABC) is an alternative method to sedimentation velocity in AUC.[11–13] ABC uses special centerpieces that have two fine capillaries connecting to a reservoir. Samples are loaded in the reservoir during cell assembly, pressured through the

Received 9 February 2021; accepted 21 April 2021;
https://doi.org/10.1016/j.omtm.2021.04.008.

Correspondence: Chunlei Wang, PhD, Analytical Sciences, Biopharmaceutical Development, AstraZeneca R&D, One MedImmune Way, Gaithersburg, MD 20878, USA.
E-mail: chunlei.wang1@astrazeneca.com

capillary channel at low rotor speed, and overlaid as a thin layer on top of the bulk solution in the centerpiece. Upon overlay, species in the sample layer start to diffuse and sediment in bands at their corresponding sedimentation velocities. Unlike SV-AUC, a physical separation of macromolecular mixtures can be achieved in ABC when there are sufficient differences in sedimentation velocities.

Vinograd et al.[13–16] pioneered ABC applications for separating macromolecules and studying their interactions in the 1960s. They studied different centerpieces and solvent pairs for optimal sample loading. They also developed mathematical models that deduce sedimentation and diffusion coefficients from ABC experiments. Since then, there have been few other reported ABC applications in literature, mostly studying interacting systems.[11,17] Schneider et al.[12] attributed the sparse adoption of ABC to the poor understanding of its initial condition from sample overlaying and the dynamic nature of solvent density and viscosity during sedimentation. They explored transforming ABC data to sedimentation boundary data and utilizing the sophisticated processing methods that had been developed for SV-AUC.[11]

In this study, we implement Vinograd's original separation methods on modern AUC instruments for pharmaceutical applications. We report using ABC separation as an alternative to SV-AUC for quantifying empty and full AAV particles. Experimental considerations and data processing approaches are presented in detail. ABC method performance and its robustness, as compared to SV-AUC, are examined for its potential routine use in quality control laboratories.

RESULTS

ABC for proteins and virus particles

Figure 1 shows typical concentration profiles of a monoclonal antibody (mAb) and an AAV during ABC experiments. Trace 1 is the first scan obtained at set rotor speed. The band widths of samples in our first scans are 940 μm for mAb and 770 μm for AAV, which are much wider than the theoretically calculated 556 μm based on 15-μL loading volume.[12] Schneider et al.[12] verified the theoretical band width on a custom-modified AUC system that can collect data during the rotor acceleration phase. In commercially available AUC systems, the sample is loaded during the acceleration phase, and band broadening occurs before the rotor reaches the desired speed, at which the first scan is measured. A mAb diffuses faster and is analyzed at higher rotor speed, because of its lower sedimentation velocity, compared to a typical AAV. As a result, its initial band width is much wider than that observed for the AAV used for this study. The concentration profiles are asymmetric at the initial measurement, with a sharp edge on the left and a diffusing concentration gradient on the right side in trace 1 (Figures 1A and 1B). Such diffusion from the sample band to the bulk solvent is compensated by density difference between solvents, which is critical to limit convection and ensure a precise and reproducible sample transfer during ABC experiments.[13] We have compared the use of sucrose, high-concentration salt, and buffer prepared using deuterium oxide (D_2O) as bulk solution. D_2O bulk solution provided faster analysis time and more reproducible results and was chosen for the rest of this study.

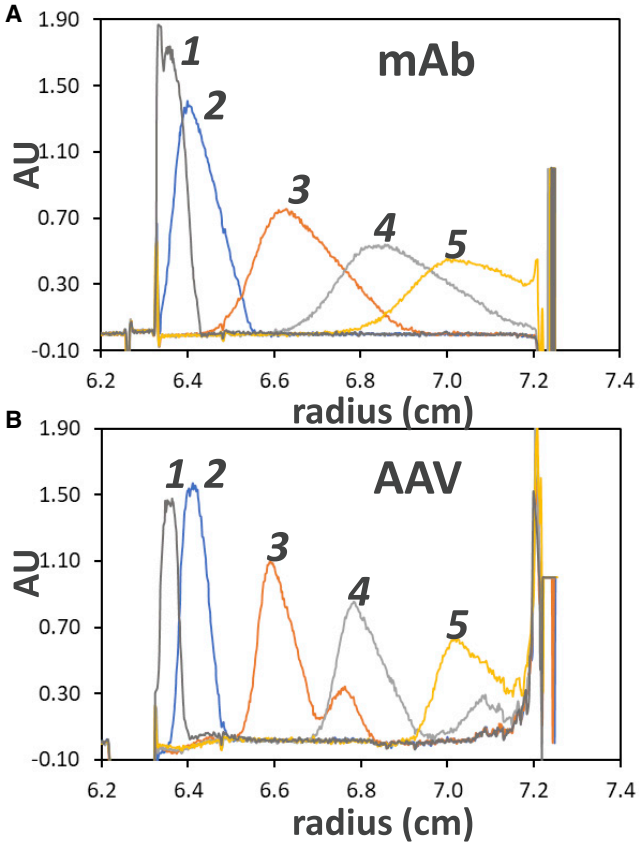

Figure 1. Concentration profiles of mAb and AAV during an ABC experiment

(A and B) Concentration profiles of a monoclonal antibody (A) and an AAV sample (B) during ABC experiments. Trace 1 is the first scan, and traces 2–5 correspond to the scans obtained when the center of the sample main band is near the radii of 6.4, 6.6, 6.8, and 7.0 cm. The y axis unit is absorbance unit (AU).

Traces 2–5 in Figure 1 are snapshots of the ABC data when the center of the sample band is near the radii of 6.4, 6.6, 6.8, and 7.0 cm, respectively. The bands display a more severe asymmetric concentration profile with a wider leading edge (right side of the peaks in Figure 1) compared to trace 1. The band width increases as they sediment to the cell bottom. Because of its higher diffusivity, slower sedimentation, and longer sedimentation time, the mAb band is approximately twice as wide as the AAV band. At the bottom of the cell, sample accumulation and back-diffusion are observed over the course of experiments.

The broadening of sedimentation bands and narrow range of sedimentation radius create practical limits for separation applications of ABC. For example, the band full width at half maximum (FWHM) of the mAb is 0.29 cm at the radius of 6.8 cm (Figure 1A, trace 4). The sedimentation velocity would need to be ~1.5× different to achieve a resolution of two species at half peak height and ~10× different to achieve baseline resolution of two species with similar diffusivity as the mAb. In the case of AAV, where diffusion is less pronounced, the FWHM is 0.12 cm at 6.8 cm (Figure 1B, trace 4), and,

therefore, the required differences in sedimentation velocity for half-peak-height and baseline resolution are ~1.3× and 1.9×, respectively.

Indeed, the two species in the AAV sample are resolved in Figure 1B, trace 3. As with any velocity-based separation, the resolution improves at longer sedimentation distance (trace 4 versus trace 3). Unfortunately, the leading edge of the small peak is cut off in trace 4 when it sediments to the bottom of the cell. Monitoring physical separation in space is thereby limited by the fastest sedimenting species.

Alternatively, ABC separations can be monitored in time at a fixed radius, which is similar to the detection window in capillary electrophoresis (CE) and liquid chromatography (LC) separations. Figure 2 shows ABC data (from the same run of Figure 1B) plotted on the time axis when detected at different radii. We dub these profiles "centrifugrams." When detecting at a larger radius, the separation improves and the peak apex intensity decreases because of band broadening.

To use centrifugraphic peaks for quantification, time correction of peak areas is required to account for different sedimentation velocities and, hence, the durations with which different species pass through the detector.[18] Using time-corrected peak areas (TCAs), peak area divided by its migration time, the calculated area percent is determined to be consistent at different radii. In the example shown in Figure 2, the mean area percent values for the two peaks are 21.1% and 78.9%, with standard deviation of 1.2% for both peaks.

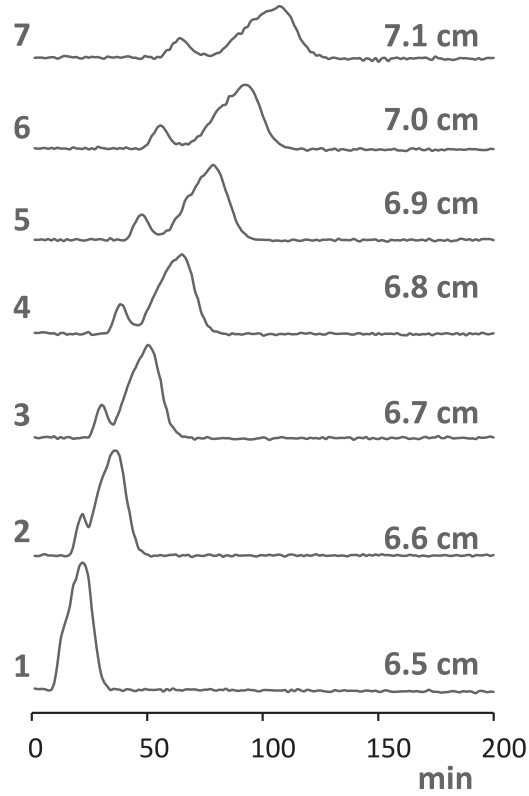

Figure 2. Centrifugrams of an ABC experiment detected at different radii
ABC experimental data (from Figure 1B) plotted on time axis when detected at different radii: traces 1–7 correspond to UV signal detected at radius of 6.5 cm with 0.1-cm increments to 7.1 cm.

Confirming AAV empty-full separation

The two species resolved by ABC in this experiment are assigned as full and empty AAV particles based on the following three observations. First, ABC separation can be monitored at multiple wavelengths, as shown in Figure S1. The first peak has a higher absorbance at 260 nm than at 280 nm, whereas the second peak has a higher 280 nm absorbance. This result suggests that the first peak contains nucleotides and proteins and the second peak is predominantly protein.[19]

Second, samples with high and low levels of full AAV particles have been analyzed by both ABC (Figures 3A and 3B) and SV-AUC (Figures 3C and 3D). The $c(s)$ of SV-AUC provides high resolution of full and empty AAV particles. Minor species corresponding to partially filled AAV and fragments were also resolved by SV-AUC (totaling $\leq$ 2.0%). Nevertheless, the area percent of first and second ABC peaks is in good agreement with that of full and empty peaks in SV-AUC. Minor differences, on the order of ~2%–4%, in the calculated full particle relative percentage are observed between the ABC and SV-AUC results.

Finally, sedimentation coefficients can be calculated using ABC data according to Equation 1.[15]

$$\ln\left(\frac{r}{r_0}\right) = s\omega^2(t - t_0) \qquad \text{(Equation 1)}$$

where r is the radius of the peak maximum, s is sedimentation coefficient, ω is angular velocity, and t is the time of measurements. By plotting $(t - t_0)$ against $\ln(r/r_0)$ using multiple data points, the s value can then be calculated from the fitted slope k using Equation 2.

$$s = \frac{1}{k\omega^2} \qquad \text{(Equation 2)}$$

Setting r_0 to 6.6 cm where the two peak apexes can be defined, the data from Figure 2 are replotted in Figure 4 for s determination. Hundreds more data points can potentially be used, but we find it sufficient to use only the six data channels at evenly spaced radii from 6.6 to 7.1 cm. The r^2 of the linear regression fit is >0.999 for both species. The determined s value for the two species are 39.1 S and 65.8 S, which matches well with the s value of empty (39.1) and full (67.6) AAV particles as experimentally determined by SV-AUC in D_2O solvents (Figure S2).

ABC method performance

Multiple experiments of the same sample (stored at 4°C) were run on two AUC instruments over a 4-month period to assess method reproducibility. Figure S3A shows the overlay of centrifugrams collected at the radius of 6.8 cm with different loading volumes (5, 7.5, 10, 12.5,

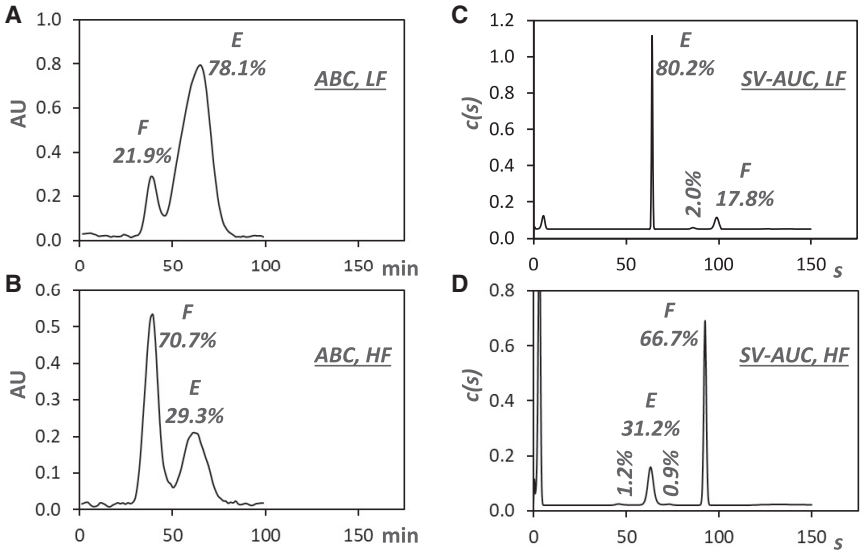

Figure 3. Comparing ABC and SV-AUC analysis of two representative AAV samples

(A–D) Results obtained using ABC (A and B) and SV-AUC (C and D) for two AAV samples: low full (LF) and high full (HF) percent particles. The ABC centrifugrams were monitored by UV 230 nm at a radius of 6.8 cm. The SV-AUC results were *c*(*s*) distribution processed using SEDFIT. Peak area percentages are labeled next to corresponding peaks: E, empty AAV particles; F, full AAV particles; a few unidentified minor peaks were also observed by SV-AUC (≤2.0%).

and 15 μL), with data for each loading volume collected twice over the 4-month period. Plotting the total peak area versus sample volume shows good linearity in the range of 5–15 μL with a r^2 of 0.9962 (Figure S3B). The difference in TCA from replicate runs is <10% at any sample loading volume. Averaging data obtained from all these experiments, the calculated area percent of the empty and full AAV particles are 78.8% and 21.2%, respectively, with a standard deviation of 1.0% (n = 10).

The performance of ABC was also evaluated using samples with different levels of full AAV particles (Figure 5). These samples were generated by mixing high and low full AAV particles at different ratios. The experimental and theoretical full AAV particle percentages showed good correlation, with a r^2 of > 0.99 and a slope of 0.99 (Figure S4), which confirms that there was no bias of response for the empty and full AAV particles using this analytical method. The range of empty or full AAV particle percentages studied was limited by the availability of more enriched samples. Assuming 1.0 absorbance unit (AU) response of the major peak, the limit of detection of the minor species (empty or full AAV particles) is estimated to be 5% based on noise level observed.

Critical method parameters in SV-AUC

SV-AUC data processing requires fitting of experimental data using the Lamm equation. Consequently, experimental parameter fluctuations or potential non-ideal sedimentation could introduce error and variation in the final results. For example, the recorded experimental times by vendor software were found to introduce up to 10% error in determination of *s* value.[20] Varying temperature would cause changes in solvent viscosity, and hence sedimentation velocity, during AUC experiments.[21] As a mitigation strategy, rotor temperature pre-equilibration (for >30 min) is a common practice for SV-AUC experiments. For example, BSA aggregation was found to increase 0.35% per degree Celsius deviation of the initial rotor temperature from the set-point.[7] Finally, cell misalignment causes observed broadening of the BSA aggregation peak in the *c*(*s*) plot. The measured aggregation level increased from 16% to 20% because of a cell misalignment of 4°.[22]

Robustness of ABC experiments

To assess the robustness of the ABC method used in this study, we evaluated the impact of the above SV-AUC critical method parameters on relative quantification of empty and full AAV particles by ABC.

In a typical ABC experiment, the average time for each scan across different radii is calculated to be 71.2 s, with a relative standard deviation (RSD) of 49% according to the experimental log data. After time correction using SEDFIT, the scan time variability is normalized throughout the experiment, with the RSD reduced to 2%. Figure S5A shows the scan time distribution before and after the SEDFIT correction. Figure S5B shows the correlation between instrument output and SEDFIT-corrected time lapse. The deviation of the trace from $y = x$ line indicates the errors in the time log. The consequence of this error is distorted peak shapes in the resulted centrifugrams, as shown in Figure S5C. This distortion is significantly reduced after time correction (Figure S5D).

As described above, temperature changes during an AUC experiment affect sedimentation velocity. Variations in temperature during ABC experiments would impact sedimentation time and, therefore, potentially impact quantification using TCA. However, the observed impact of significant temperature fluctuation during ABC experiments on the AAV relative quantification results was shown to be negligible. To determine this impact, we started the ABC experiment with the initial temperature 5°C above the setpoint of 20°C. The temperature log is plotted in Figure S6. The area percent result of the full AAV particle was determined to be 22.0%, which is similar to the result, 21.2%, obtained with no initial temperature deviation. Surprisingly, even the calculated *s* values were not affected by this 5°C temperature deviation when determined using Equations 1 and 2. This result is likely because the initial sedimentation behavior, at radius < 6.6 cm, during ABC is not used for our *s* value calculations. The rotor temperature dropped to 22°C when the center of the full AAV particle traveled to the radius of 6.6 cm (Figure S6). The temperature further

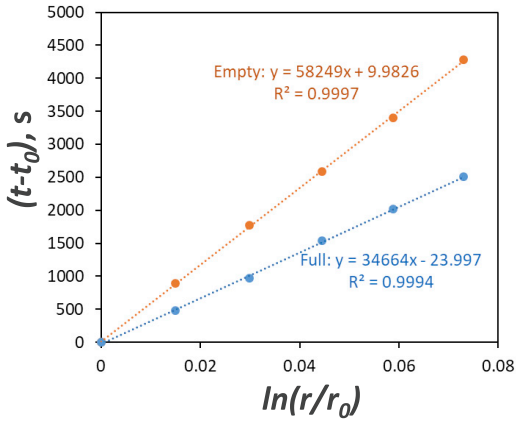

Figure 4. Linear regression for sedimentation coefficient determination by ABC experiments

ABC data were processed for linear fitting of $(t - t_0)$ ~$\ln(r/r_0)$. The slope was used for sedimentation velocity determination according to Equation 2.

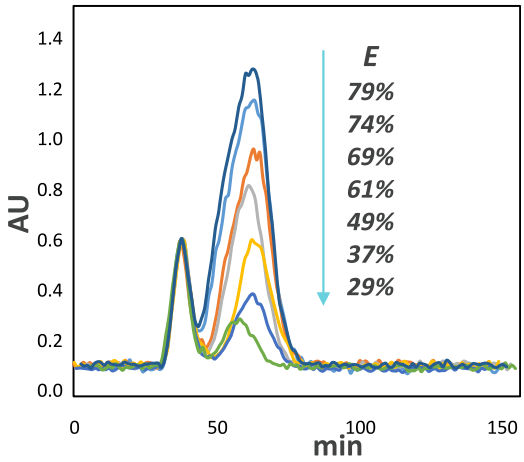

Figure 5. ABC centrifugrams of AAV samples with different percentage of empty particles

ABC centrifugram overlay of AAV samples with different percentages of empty particles (calibration range shown in Figure S4). The centrifugrams were normalized and aligned to the full AAV particle peak (front peak). The expected empty capsid percentage is also listed.

dropped to within 1°C and 0.5°C of the setpoint when the leading band traveled to 6.7 and 6.8 cm, respectively. Additionally, the linear fitting approach to determine sedimentation coefficients is less susceptible to minor data deviations occurring at smaller radii.

The alignment of sample cells to the center of rotation was determined to be the most significant contributor to SV-AUC method variability.[7] To evaluate the impact of cell misalignment for ABC experiments, we tested cell misalignment at +5° and −5° (Figure S7). The area percent results of the full AAV particle were determined to be 21.5% and 20.3%, respectively. Both results are within one standard deviation from 21.2%, which is obtained using perfectly aligned cells.

Figure 6 shows the overlay of five ABC centrifugrams, including duplicate measurements using correct experimental settings, one measurement with starting rotor temperature offset by 5°C, and two measurements with cell misaligned by +5° and −5°. The raw scans of these experiments are shown in Figure S8. The centrifugrams obtained from temperature and cell alignment deviation studies cannot be differentiated from replicates generated using the desired target experimental settings. Summarizing all conditions in Figure 6, the RSD of total area with a 15-μL sample loading is 5.2%. Figure 7 compiles the area percent and *s* value of both empty and full AAV particles from all experiments discussed in this study. Area percent results for all experiments fall within one standard deviation, except for the 5-μL sample, which is close to the detection limit. The *s* value also showed good reproducibility across all experiments. The cell misalignment seems to have a slight impact on the calculated *s* value. In summary, neither area percent nor sedimentation coefficients were adversely impacted by practical deviations of initial temperature or cell alignment during ABC experiments.

DISCUSSION

We evaluated ABC for the separation of macromolecules. Proteins of ~150 kDa size, such as mAbs, diffuse quickly into broad bands during sedimentation. Given the short sedimentation radius range, it is challenging to resolve any product-related size or mass variants for mAbs. On the other hand, AAV virus particles, which sediment faster and diffuse slower, form narrower bands during ABC experiments. Empty and full AAV particles can be physically separated because of large differences in their sedimentation velocities.

The AAV separations during ABC experiments can be monitored at a fixed radius. The resulting centrifugrams can be processed in a similar

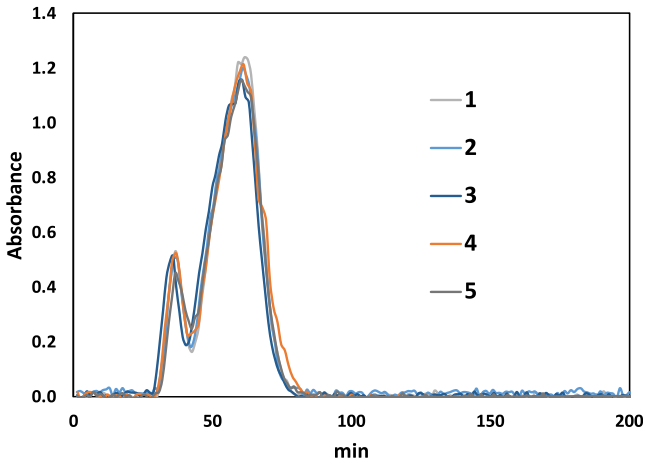

Figure 6. Robustness of ABC experiments

Overlay of replicates of ABC experiments under normal condition and several deviation conditions: traces 1 and 2, replicates of normal conditions; trace 3, starting temperature is 5°C above experimental setting; traces 4 and 5, cell misaligned at +5° and −5°.

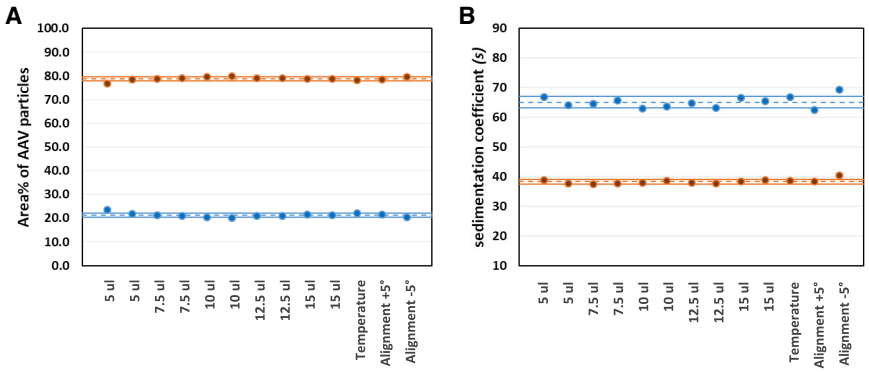

Figure 7. Monitoring of ABC experimental results for all experiments during the course of this study

(A) Peak area percent. (B) Sedimentation coefficients. The results for empty and full AAV particles are presented by orange and blue dots, respectively. The dotted lines are average values, and solid lines are boundary lines defined as the mean values ± one standard deviation. The x axis lists experimental conditions including different sample volumes in replicates (5, 7.5, 10, 12.5, and 15 μL), temperature deviation experiment that started from +5°C above set temperature, and cell alignment experiments in which cell was purposely misaligned at ±5°. A sample volume of 15 μL was used for temperature and alignment deviation experiments.

way as in CE. Time-corrected area can be used for relative quantification of empty and full AAV particles. Additionally, sedimentation coefficients can be determined through linear fitting of band position data at different time points.

The empty and full AAV particle percentages and sedimentation coefficients determined by ABC and SV-AUC are comparable. The $c(s)$ results produced from SV-AUC give much higher resolution between empty and full AAV particles. SV-AUC is also more tolerant for low-concentration samples. On the other hand, ABC requires a minimum AAV viral titer of ~5×10^{11} vg/mL but uses 5% of the sample volume needed for SV-AUC. The ABC experimental time and data processing time are both shorter than for SV-AUC.

The processing of ABC data from AAV separations does not include any subjective steps, such as meniscus determination required during SV-AUC data analysis, nor does it require a complicated optimization algorithm or sophisticated software packages. The Python scripts developed in-house were used simply to streamline data extraction, integration, and reporting. As a result, the processing step is not expected to introduce any variability in final results.

Additionally, the ABC experiments are more tolerant than SV-AUC to variation of experimental parameters. SV-AUC requires near-ideal sedimentation behavior in order to fit data into the theoretical Lamm equation. Experimental parameter settings in SV-AUC need to be well controlled to ensure SV-AUC method reproducibility. In contrast, we found that ABC methods are more robust. Deviation of 5°C in initial temperature or ±5° in cell alignment does not impact peak area or its percentages in ABC separations.

In conclusion, we have evaluated the use of ABC for the separation and quantification of empty and full AAV particles. The ABC experimental raw data are directly used for peak presentation and integration with no need for complicated optimization steps. Good reproducibility and robustness have been demonstrated for calculation of both relative peak percentage and sedimentation coefficients in ABC experiments. Given these desirable attributes, ABC could become a promising technique for routine analysis of therapeutic AAV products. Additionally, the ABC application on AAVs can potentially be extended to the characterization of other viral and vaccine products.

MATERIALS AND METHODS

AAV vectors were produced in-house as described previously.[4] Chemical reagents, including buffers and D_2O (catalog number 151882), were purchased from Sigma-Aldrich (St. Louis, MO, USA).

SV-AUC experiments were performed on a Beckman Coulter ProteomeLab XL-I instrument (Beckman Coulter, Indianapolis, IN, USA) using standard Beckman Coulter cells equipped with 12-mm, two-sector centerpieces and Sapphire windows. 400 μL of sample and 410 μL of buffer (same as sample buffer, pH 7.0) were loaded in the sample and reference sectors, respectively, prior to analysis. After the cell was fixed into an eight-cell rotor and mounted in the instrument, it was allowed to equilibrate for 1 h after reaching vacuum and the set temperature of 20°C. The sample was then centrifuged at 20,000 rpm rotor speed while the absorbance signal was collected at 230 nm for 200 scans in the radius range of 6.15–7.25 cm. The wavelength of 230 nm was selected for better sensitivity and less response bias between empty and full AAV capsids. The SV-AUC data were processed with SEDFIT[23] software, following a previously published approach.[5]

For ABC experiments, band forming centerpieces (Spin Analytical, South Berwick, ME, USA) with two sectors and a 15-μL sample reservoir were used to assemble the cells. Various volumes (up to 15 μL) were loaded to the sample reservoir prior to cell assembly. 330 μL and 290 μL of running buffer (same as sample buffer but prepared in D_2O, pH 7.0) were loaded in the reference sector and sample sector, respectively. All other experimental procedure and setups are identical to SV-AUC experiments.

The ABC data processing was facilitated by in-house Python scripts after time correction using SEDFIT. Specifically, the absorbance data at a corresponding radius were extracted to produce the intensity versus time plot. The peak integration and quantification was built upon the open source *peakdetect* Python package. The sedimentation

coefficient was determined using peak apex and its corresponding time at various radii. The Python source code is available upon request.

SUPPLEMENTAL INFORMATION

Supplemental information can be found online at https://doi.org/10.1016/j.omtm.2021.04.008.

ACKNOWLEDGMENTS

The authors would like to thank Guoling Xi and Dr. Thomas Linke for providing AAVs for this study. We also thank Yoen Joo Kim and Dr. Albert E. Schmelzer for critical review of the manuscript. This research was developed with funding from the Defense Advanced Research Projects Agency under HR011-18-3-001. The views, opinions, and/or findings expressed are those of the authors and should not be interpreted as representing the official views or policies of the Department of Defense or the US government.

AUTHOR CONTRIBUTIONS

Conceptualization and methodology, C.W.; investigation, H.K. and C.W.; writing – original draft, C.W.; writing – review & editing, H.K., G.K., X.C., and C.W.

DECLARATION OF INTERESTS

All authors are employees of AstraZeneca PLC.

REFERENCES

1. Wang, D., Tai, P.W.L., and Gao, G. (2019). Adeno-associated virus vector as a platform for gene therapy delivery. Nat. Rev. Drug Discov. *18*, 358–378.
2. Flotte, T.R. (2017). Empty adeno-associated virus capsids: Contaminant or natural decoy? Hum. Gene Ther. *28*, 147–148.
3. Wright, J.F. (2014). AAV empty capsids: for better or for worse? Mol. Ther. *22*, 1–2.
4. Wang, C., Mulagapati, S.H.R., Chen, Z., Du, J., Zhao, X., Xi, G., Chen, L., Linke, T., Gao, C., Schmelzer, A.E., and Liu, D. (2019). Developing an anion exchange chromatography assay for determining empty and full capsid contents in aav6.2. Mol. Ther. Methods Clin. Dev. *15*, 257–263.
5. Burnham, B., Nass, S., Kong, E., Mattingly, M., Woodcock, D., Song, A., Wadsworth, S., Cheng, S.H., Scaria, A., and O'Riordan, C.R. (2015). Analytical ultracentrifugation as an approach to characterize recombinant adeno-associated viral vectors. Hum. Gene Ther. Methods *26*, 228–242.
6. Brown, P.H., and Schuck, P. (2008). A new adaptive grid-size algorithm for the simulation of sedimentation velocity profiles in analytical ultracentrifugation. Comput. Phys. Commun. *178*, 105–120.
7. Arthur, K.K., Gabrielson, J.P., Kendrick, B.S., and Stoner, M.R. (2009). Detection of protein aggregates by sedimentation velocity analytical ultracentrifugation (SV-AUC): sources of variability and their relative importance. J. Pharm. Sci. *98*, 3522–3539.
8. Pekar, A., and Sukumar, M. (2007). Quantitation of aggregates in therapeutic proteins using sedimentation velocity analytical ultracentrifugation: practical considerations that affect precision and accuracy. Anal. Biochem. *367*, 225–237.
9. Zhao, H., Ghirlando, R., Alfonso, C., Arisaka, F., Attali, I., Bain, D.L., Bakhtina, M.M., Becker, D.F., Bedwell, G.J., Bekdemir, A., et al. (2015). A multilaboratory comparison of calibration accuracy and the performance of external references in analytical ultracentrifugation. PLoS ONE *10*, e0126420.
10. Savelyev, A., Gorbet, G.E., Henrickson, A., and Demeler, B. (2020). Moving analytical ultracentrifugation software to a good manufacturing practices (GMP) environment. PLoS Comput. Biol. *16*, e1007942.
11. Schneider, C.M., and Cölfen, H. (2018). Analytical band centrifugation revisited. Eur. Biophys. J. *47*, 799–807.
12. Schneider, C.M., Haffke, D., and Cölfen, H. (2018). Band sedimentation experiment in analytical ultracentrifugation revisited. Anal. Chem. *90*, 10659–10663.
13. Vinograd, J., Bruner, R., Kent, R., and Weigle, J. (1963). Band-centrifugation of macromolecules and viruses in self-generating density gradients. Proc. Natl. Acad. Sci. USA *49*, 902–910.
14. Vinograd, J., Radloff, R., and Bruner, R. (1965). Band-forming centerpieces for the analytical ultracentrifuge. Biopolymers *3*, 481–489.
15. Vinograd, J., and Bruner, R. (1966). Band centrifugation of macromolecules in self-generating density gradients. Ii. Sedimentation and diffusion of macromolecules in bands. Biopolymers *4*, 131–156.
16. Vinograd, J., and Bruner, R. (1966). Band centrifugation of macromolecules in self-generating density gradients. Iii. Conditions for convection-free band sedimentation. Biopolymers *4*, 157–170.
17. Lebowitz, J., Teale, M., and Schuck, P.W. (1998). Analytical band centrifugation of proteins and protein complexes. Biochem. Soc. Trans. *26*, 745–749.
18. Chamieh, J., Martin, M., and Cottet, H. (2015). Quantitative analysis in capillary electrophoresis: transformation of raw electropherograms into continuous distributions. Anal. Chem. *87*, 1050–1057.
19. Sommer, J.M., Smith, P.H., Parthasarathy, S., Isaacs, J., Vijay, S., Kieran, J., Powell, S.K., McClelland, A., and Wright, J.F. (2003). Quantification of adeno-associated virus particles and empty capsids by optical density measurement. Mol. Ther. *7*, 122–128.
20. Zhao, H., Ghirlando, R., Piszczek, G., Curth, U., Brautigam, C.A., and Schuck, P. (2013). Recorded scan times can limit the accuracy of sedimentation coefficients in analytical ultracentrifugation. Anal. Biochem. *437*, 104–108.
21. Ghirlando, R., Balbo, A., Piszczek, G., Brown, P.H., Lewis, M.S., Brautigam, C.A., Schuck, P., and Zhao, H. (2013). Improving the thermal, radial, and temporal accuracy of the analytical ultracentrifuge through external references. Anal. Biochem. *440*, 81–95.
22. Channell, G., Dinu, V., Adams, G.G., and Harding, S.E. (2018). A simple cell-alignment protocol for sedimentation velocity analytical ultracentrifugation to complement mechanical and optical alignment procedures. Eur. Biophys. J. *47*, 809–813.
23. Schuck, P. (2000). Size-distribution analysis of macromolecules by sedimentation velocity ultracentrifugation and lamm equation modeling. Biophys. J. *78*, 1606–1619.